

4. $^{40}\text{Ar}/^{39}\text{Ar}$ GEOCHRONOLOGY OF BASEMENT ROCKS FROM THE MASCARENE PLATEAU, THE CHAGOS BANK, AND THE MALDIVES RIDGE¹

Robert A. Duncan² and Robert B. Hargraves³

ABSTRACT

Concordant plateau and isochron ages were calculated from $^{40}\text{Ar}/^{39}\text{Ar}$ incremental heating experiments on volcanic rocks recovered by drilling at four Leg 115 sites and two industry wells along the volcanic lineament connecting Réunion Island to the Deccan flood basalts, western Indian Ocean. The new ages provide unequivocal evidence that volcanic activity migrated southward along this sequence of linear ridges. The geometry and age distribution of volcanism are most compatible with origin above a stationary hotspot centered beneath Réunion. The hotspot became active with rapid eruption of the Deccan flood basalts, western India, and subsequent volcanic products record the northward motion of the Indian and African plates over the hotspot through Tertiary time. The radiometric ages are in general accord with basal biostratigraphic age estimates, although some adjustments in current magnetobiostratigraphic time scales may be required.

INTRODUCTION

One of the remarkable features of the floor of the Indian Ocean is the large number of elevated plateaus, banks, and ridges scattered throughout the basin. The origins of these bathymetric elements have been ascribed to continental fragments left behind in Gondwana separation, to ancient foundered island arcs, and to volcanic activity associated with either fracture zones cutting the oceanic lithosphere or stationary hotspots. The Seychelles Islands, at the northwestern end of the Mascarene Plateau (Fig. 1), are composed of late Precambrian granites and dolerites that are intruded by Late Cretaceous/early Tertiary basaltic dikes and ring complexes (Baker and Miller, 1963; Macintyre et al., 1988; Hargraves and Duncan, this volume). The arcuate shape of the combined Mascarene and Seychelles plateaus led Meyerhoff and Kamen-Kaye (1981) to propose that these were underlain by a Paleozoic island arc. McKenzie and Sclater (1971) noted that the Mascarene Plateau, the Chagos Bank, and the Maldives-Laccadive ridges were collinear prior to Neogene seafloor spreading at the Central Indian Ridge; they proposed that this lineament was formed by volcanic activity along a north-south transform fault related to early Tertiary opening of the Indian Ocean.

Morgan (1981) and Duncan (1981) showed that the location and orientation of these same western Indian Ocean ridges are those expected from calculated motions of the Indian and African plates over the Réunion hotspot. The hotspot is thought to be a region of excess melting of the upper mantle that persists at a stationary location because it is supplied by a stable, convective plume of hot material rising from lower in the mantle (Morgan, 1972). Buoyant melts from the hotspot penetrate the overlying lithosphere, and the resulting volcanic activity builds lineaments consisting of discrete volcanoes and volcanic ridges. According to this model, then, these volcanic trails record the motion of the plates surrounding the Indian Ocean.

Morgan (1981) proposed that young volcanic activity at the island of Réunion is the present manifestation of a stationary hotspot that earlier produced the island of Mauritius, the volcanic ridge underlying much of the Mascarene Plateau, the Chagos Bank, and the Maldives and Laccadive islands. The initial phase of hotspot activity probably occurred with the eruption of massive volumes of flood basalts of the Deccan Traps, western India (Fig. 1). Northward motion of the Indian Plate, followed by northeastward motion of the African plate, over a hotspot beneath Réunion would have left the observed volcanic trail. In addition, the Ninetyeast Ridge is another parallel submarine volcanic lineament linked to hotspot activity, now centered near the Kerguelen Islands, Antarctic plate, and these two track the northward motion of India during the opening of the Indian Ocean.

Precise radiometric dating of the basement rocks forming these ridges is critical in distinguishing the competing genesis models. An explicit prediction of the hotspot model is that all basement ages be younger than the Deccan flood basalts and become progressively younger from the northern to the southern end of the lineament. Other models predict either sporadic or synchronous volcanism along the line (McKenzie and Sclater, 1971) or pre-Tertiary ages. Until Leg 115 the only accessible sampling locations along this ridge system were at the end points: the young volcanic islands to the south and the Late Cretaceous/early Tertiary Deccan flood basalts to the north. During Leg 115 volcanic rocks were recovered by drilling at four intermediate sites along this trace. In addition, we have received volcanic samples from two oil industry exploration wells drilled into the Mascarene Plateau. In this paper we report the results of $^{40}\text{Ar}/^{39}\text{Ar}$ incremental heating experiments on volcanic rocks from these six sites, which establish an unequivocal north-to-south age progression and support the proposed hotspot origin for this prominent lineament.

ELEMENTS OF THE REUNION HOTSPOT TRACK

The Mascarene Islands: Réunion, Mauritius, and Rodrigues

The volcanic islands of Réunion, Mauritius, and Rodrigues (collectively called the Mascarene Islands) lie between 19° and 22°S and between 55° and 64°E at the southern end of the volcanic lineament (Fig. 1). Réunion Island rises 7000 m from an

¹ Duncan, R. A., Backman, J., Peterson, L. C., et al., 1990. *Proc. ODP, Sci. Results*, 115: College Station, TX (Ocean Drilling Program).

² College of Oceanography, Oregon State University, Corvallis, OR 97331, U.S.A.

³ Department of Geological and Geophysical Sciences, Princeton University, Princeton, NJ 08544, U.S.A.

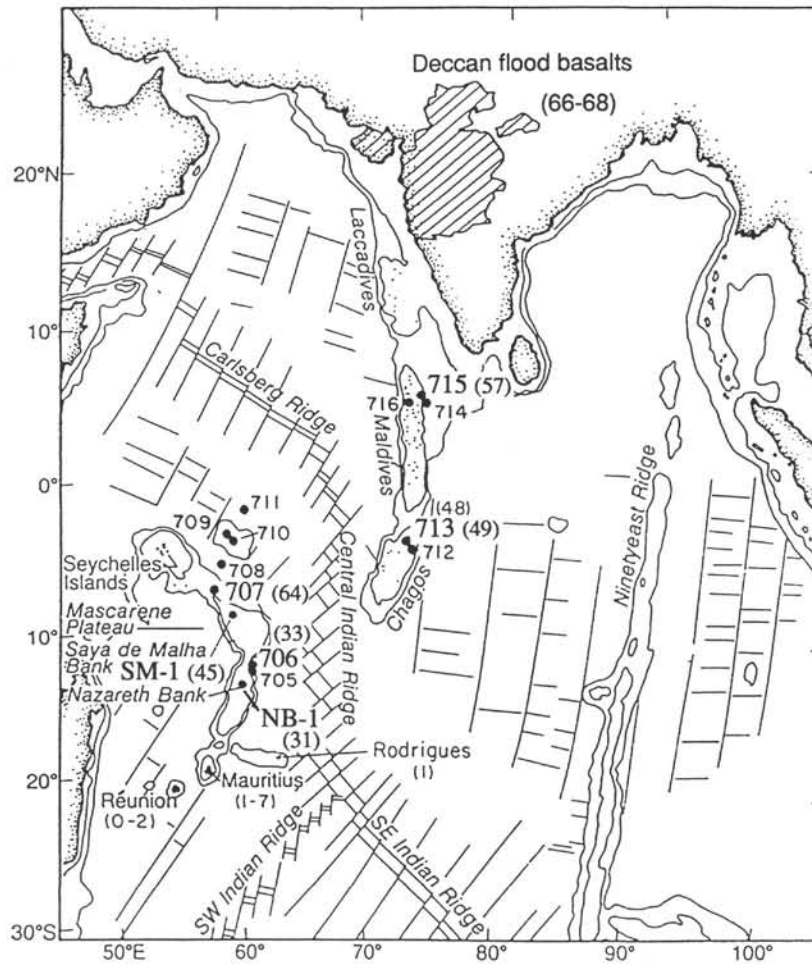


Figure 1. Bathymetric features of the central Indian Ocean. The Réunion hotspot track includes the Nazareth, Saya de Malha, and Chagos banks, the Maldives and Laccadives ridges, and the Deccan flood basalts. Leg 115 drilling sites are shown; those in which basaltic basement was recovered are enlarged, as are industry well sites on the Mascarene Plateau. The best radiometric age estimates are indicated in parentheses.

ocean floor of Paleocene age (Chron 27 = 63 Ma; Berggren et al., 1985a). The island is formed of two coalesced volcanoes: Piton des Neiges, which is inactive and forms the northwest two-thirds of the island, and the active Piton de la Fournaise, 30 km away, which forms the southeastern part of the island. McDougall (1971) has established the age relationships of volcanism within the Mascarene Islands. The oldest rocks found at Réunion are about 2 Ma. Piton des Neiges has not been active for the last 70,000 yr, whereas Piton de la Fournaise began erupting about 360,000 yr ago. From the volume of volcanic material forming the island (~75,000 km³), we calculate an average eruption rate of 0.04 km³/yr for this most recent site of hotspot activity. We note, however, the presence of a large seamount some 160 km west of Réunion that may be the newest volcano in the trace.

Mauritius, an eroded volcanic island to the northeast of Réunion, was built by perhaps three eruptive episodes (McDougall, 1971). The first, most voluminous phase built the original shield volcano at 7–8 Ma. Later stages of volcanic activity occurred at 2–3.5 Ma and 0.2–0.7 Ma. The cause of these “rejuvenescent” phases of volcanism may seem perplexing in terms of a simple hotspot model, for if the ages of the initial (main) shield-building stage of island formation mark the time of location over the hotspot, then the subsequent volcanism must de-

rive from melts erupted when the island was several hundred kilometers downstream from the hotspot. The long thermal response time of oceanic lithosphere, however, may mean that once volcanism is initiated at a site, activity may recur long afterward, even if the hotspot heat source has moved away.

Rodrigues Island lies about halfway between Mauritius and the Central Indian spreading ridge, at the eastern end of the east-west Rodrigues Ridge. The island is composed of olivine basalts that erupted about 1.5 Ma (McDougall, 1971). It is now known from extensive dredging and surveying (*Darwin* 21/87 site survey cruise for Leg 115) that the Rodrigues Ridge is entirely volcanic. The age of the island and the position of the Rodrigues Ridge, east of the Mauritius-Mascarene Plateau trend, also present a puzzle if this volcanic feature is part of the hotspot track.

Morgan (1978) has proposed that the Rodrigues Ridge, and similar features such as the Darwin-Wolf Island lineament north of the Galapagos Islands, result from “channelized” asthenospheric flow from the hotspot to a nearby spreading ridge. The trend of the Rodrigues Ridge does not have any apparent relationship to transform faults or old spreading segments formed at the Central Indian Ridge. Instead, its orientation may derive from the vector sum of African Plate motion plus the relative motion of the spreading ridge.

Industry Wells on the Mascarene Plateau

The morphology and surface geology of the Mascarene Plateau have been discussed by Fisher et al. (1967). Drilling has now established that these shallow carbonate banks are fundamentally volcanic ridges that originally rose above or very near sea level and have subsided slowly enough to allow coral growth to flourish. Meyerhoff and Kamen-Kaye (1981) described the stratigraphy at two test wells drilled by Texaco, Inc., in 1975 on the Saya de Malha Bank (SM-1) and the Nazareth Bank (NB-1), Mascarene Plateau (Fig. 1). At the northern site (SM-1), 2400 m of late Paleocene to Quaternary, neritic to shallow-water carbonate rocks overlie a 830-m drilled section of olivine tholeiitic basalts. The mineralogy of the basaltic chips recovered is described by Fisk and Howard (this volume). Conventional K-Ar analyses yielded Miocene ages for these altered basalts (reported in Meyerhoff and Kamen-Kaye, 1981). At the Nazareth Bank site (NB-1), drilling reached a total depth of 1700 m, the lower 160 m of which were basalts and trachytic rocks. The overlying sedimentary sequence was Oligocene to Pliocene shallow-water carbonates. Late Oligocene K-Ar ages (~25 Ma) have been reported for this volcanic material.

Sites Drilled During Leg 115

Deep-sea drilling during Leg 115 recovered basaltic rocks from four locations: (1) Site 706, at the northern margin of Nazareth Bank; (2) Site 707, on the saddle between the Seychelles and Saya de Malha banks; (3) Site 713, at the northern edge of Chagos Bank; and (4) Site 715, on the northeastern margin of the Maldives Ridge (Fig. 1). The following basement penetrations (and basalt recoveries) were achieved: Site 706, 77 m (20 m); Site 707, 63 m (39 m); Site 713, 85 m (42 m); and Site 715, 77 m (30 m). The rocks are primarily tholeiitic oceanic-island basalts and vary from aphyric to plagioclase-phyric and (rarely) olivine-phyric types.

Lavas at Site 715 were erupted subaerially, whereas those at Sites 706 and 713 accumulated under shallow marine conditions; Site 707 basalts formed subaerially or in very shallow water, the paucity of high-temperature oxidation of magnetic minerals suggesting the latter. Descriptions of cored material, including shipboard lithologic, petrographic, and X-ray fluorescence (XRF) major and trace element analyses, have appeared in the *Proceedings of the Ocean Drilling Program, Initial Reports for Leg 115* (Backman, Duncan, et al., 1988), and additional detailed compositional and mineralogical data are presented elsewhere in this volume.

The Deccan Flood Basalts

At the northern end of the proposed Réunion hotspot track is the remarkable Deccan flood basalt province, covering over 500,000 km² of west and central India. In places, the basalt flows form sequences more than 2000 m thick. The original volume of these subaerially erupted basalts may have exceeded 1.5×10^6 km³ (Mahoney, 1988). These are predominantly tholeiitic basalts, although alkali basalts were erupted in the waning stages of volcanic activity. Excellent summaries of the stratigraphy and geochemical composition of the Deccan basalts have appeared recently (Cox and Hawkesworth, 1985; Beane et al., 1986; Mahoney, 1988).

Recent high-precision radiometric dating places the age of the Deccan volcanism between 64 and 69 Ma (Duncan and Pyle, 1988; Courtillot et al., 1988; Pande et al., 1988). Magnetostratigraphic data have been used to argue that the entire sequence was erupted over two reversals of the magnetic field (Courtillot et al., 1986). In this case, the whole eruptive history would cover only 1 m.y. or less. The age and duration of the Deccan flood basalt volcanism is important in the context of initiation of hot-

spot activity (Richards et al., 1989) and the position of India at Late Cretaceous/early Tertiary time.

SAMPLE SELECTION AND ANALYTICAL METHODS

Cuttings collected at 10-m intervals during drilling at well site SM-1 were examined petrographically. These small (1–2 mm) basalt chips were moderately to extensively altered; reasonably fresh, euhedral phenocrysts of plagioclase and clinopyroxene are surrounded by groundmass totally replaced by low-temperature secondary minerals (clays, zeolites, calcite). Rare relict olivine phenocrysts have been altered to clays. Two bulk samples (from 3246 and 3292 mbsf) were handpicked to obtain 1–2 g of the freshest chips for age determinations. The chips were ultrasonically washed in water to remove drilling mud and then washed in 5% HNO₃ for 30 min to remove much of the poorly crystallized groundmass alteration. One 5 cm in diameter, cored piece of fresh-looking trachytic rock from the bottom of the NB-1 well was crushed to 0.5–1-mm size chips and ultrasonically washed in water only.

Only the freshest and best crystallized material from the centers of large pieces of core (flow interiors) were selected from samples from the four Leg 115 basement sites during a visual inspection of cores on board ship. Secondary criteria used in choosing material stipulated that samples come from flows with the highest K₂O available and flows that represented distinct compositional basalt types, as determined from shipboard XRF analyses. These samples were crushed to 0.5–1-mm sizes and were ultrasonically washed in water.

For samples analyzed at Oregon State University, approximately 1-g splits of the prepared chips were sealed in evacuated quartz tubes and irradiated for 10–15 hr in the core of the Oregon State University TRIGA reactor, where they received a neutron dose of $1.0\text{--}1.5 \times 10^{18}$ nvt. Those samples analyzed at Princeton University were first wrapped in aluminum foil and irradiated for 12 hr at the McMaster University reactor; they received a neutron dose similar to the samples analyzed at Oregon State. The efficiency of conversion of ³⁹K to ³⁹Ar by neutron capture was monitored for both the Oregon State and Princeton experiments, with samples of hornblende standard Mmhb-1 (520 Ma; Samson and Alexander, 1987). Further details of the flux characteristics, monitor minerals, sample loadings, and the corrections for interfering K- and Ca-derived Ar isotopes are given by Dalrymple et al. (1981) for the TRIGA reactor and Masliwec (1981) for the McMaster reactor.

Argon extractions for the incremental heating experiments at Oregon State University were performed in a conventional glass extraction line using radio-frequency induction heating following bake-out at 180°C (Dalrymple and Lanphere, 1969). Heating steps were set from power levels on the generator and were those determined from previous experience that divided the total sample argon into roughly equal portions. Samples were held at each step setting (temperature) for 30 min. Experiments done at Princeton used a similar glass extraction system but with a Lindbergh convection furnace. Between 6 and 12 steps were extracted from each sample. The argon composition of each gas increment was measured mass spectrometrically at Oregon State with an AEI MS-10S instrument and at Princeton with a MAT GD 150 instrument.

After corrections for background, mass fractionation, and isotopic interferences, the ⁴⁰Ar/³⁹Ar incremental heating data were reduced as both age spectra and ³⁶Ar/⁴⁰Ar vs. ³⁹Ar/⁴⁰Ar isochrons; the results appear in Table 1 and Figures 2–7. For the analyses at Oregon State University, the system background was 5×10^{-16} moles ³⁶Ar and sample sizes varied between 0.8 and 1.2 g; individual step ⁴⁰Ar/³⁶Ar compositions can be estimated from the isochron plots. For the analyses at Princeton Univer-

Table 1. $^{40}\text{Ar}/^{39}\text{Ar}$ plateau and isochron ages for basalts from the Réunion hotspot track.

Core, section, interval (cm)	Plateau age $\pm 1\sigma$ (Ma)		Integrated age (Ma)	^{39}Ar (% of total)	Isochron age $\pm 1\sigma$ (Ma)	<i>N</i>	SUMS (<i>N</i> - 2)	$^{40}\text{Ar}/^{36}\text{Ar}$ intercept
	Wgt by $1/\sigma^2$	Wgt by % ^{39}Ar						
Oregon State University:								
115-706C-2R-2, 63-66	33.1 \pm 0.3	33.3 \pm 0.5	32.5 \pm 0.7	42	34.1 \pm 2.2	5	4.2	280.5 \pm 20.9
115-706C-5R-1, 71-74	34.2 \pm 0.5	34.7 \pm 1.7	31.0 \pm 3.0	62	32.8 \pm 0.8	4	0.3	299.4 \pm 4.8
115-706C-8R-3, 51-55	32.8 \pm 1.1	33.2 \pm 1.7	33.5 \pm 0.4	57	30.5 \pm 2.0	6	0.7	287.2 \pm 5.2
115-707C-26R-5, 110-113	63.9 \pm 2.2	63.3 \pm 1.3	61.6 \pm 3.8	76	64.1 \pm 1.1	4	0.2	294.9 \pm 2.7
115-713A-13R-2, 142-144	50.9 \pm 3.5	49.8 \pm 3.7	53.2 \pm 1.6	89	42.7 \pm 5.3	4	3.7	298.3 \pm 3.1
115-713A-15R-5, 62-65	49.4 \pm 1.2	49.0 \pm 1.1	53.8 \pm 2.4	86	49.6 \pm 2.5	6	1.5	296.9 \pm 1.8
115-713A-18R-1, 27-30	48.9 \pm 3.3	49.0 \pm 5.4	47.5 \pm 5.3	100	50.5 \pm 1.4	6	2.7	292.4 \pm 2.1
115-713A-19R-1, 71-73	48.1 \pm 2.8	48.0 \pm 3.1	50.4 \pm 2.3	81	51.9 \pm 2.8	5	0.2	294.6 \pm 1.9
115-715A-30R-5, 132-135	55.6 \pm 0.9	56.1 \pm 2.2	55.3 \pm 1.6	86	55.5 \pm 4.5	7	1.6	295.6 \pm 1.0
SM-1-1, 10,700'	44.7 \pm 0.4	44.8 \pm 2.1	53.4 \pm 1.8	60	47.4 \pm 4.1	4	4.8	301.3 \pm 14.0
SM-1-2, 10,500'	51.9 \pm 0.6	49.0 \pm 4.8	59.3 \pm 1.1	69	47.7 \pm 8.0	4	9.0	301.9 \pm 3.6
NB-1, 5626'	31.5 \pm 0.1	31.5 \pm 0.2	31.5 \pm 0.2	100	31.5 \pm 0.3	4	0.6	295.5 \pm 8.4
Princeton University:								
115-706C-5R-1, 85-90	39.0 \pm 1.8	34.8 \pm 6.3	29.9 \pm 2.7	57	34.9 \pm 2.0	7	0.7	281.1 \pm 34.5
115-707C-25R-1, 104-106	73.1 \pm 4.2	72.8 \pm 7.6	59.3 \pm 3.8	60	74.3 \pm 11.0	4	1.3	294.3 \pm 6.6
115-707C-28R-4, 133-136	58.3 \pm 1.4	56.2 \pm 5.5	44.6 \pm 3.4	70	63.3 \pm 3.7	6	6.9	280.0 \pm 8.4
115-713A-15R-4, 43-47	50.0 \pm 2.1	49.3 \pm 5.4	43.2 \pm 2.3	59	49.3 \pm 3.1	6	1.9	298.3 \pm 6.2
115-715A-26R-2, 12-15	57.0 \pm 1.1	58.1 \pm 3.6	61.0 \pm 2.2	65	57.6 \pm 3.8	8	1.9	294.2 \pm 10.8
115-715A-29R-2, 32-35	58.8 \pm 1.9	65.2 \pm 9.5	61.1 \pm 2.0	85	59.7 \pm 4.8	9	1.4	306.9 \pm 15.7

sity, the system background was 7×10^{-17} moles ^{36}Ar (at 500°C) to 7×10^{-16} moles ^{36}Ar (at 1200°C) and 1-g sample sizes were used. Complete incremental heating data as well as additional plateau and $^{36}\text{Ar}/^{40}\text{Ar}$ vs. $^{39}\text{Ar}/^{40}\text{Ar}$ isochron diagrams can be obtained upon request from the authors. Apparent Ca/K ratios were calculated for each step argon composition using the relationship $\text{Ca}/\text{K} = 1.852 \text{ }^{37}\text{Ar}/^{39}\text{Ar}$ mol/mol (Walker and McDougall, 1982).

We selected steps to be integrated for plateau ages if they formed a well-defined, high-temperature age spectrum of three or more contiguous heating increments, with calculated ages that were statistically indistinguishable ($\pm 1\sigma$). We combined the step ages to calculate plateau ages in two ways (Table 1). First, we followed the method of Dalrymple et al. (1988) in weighting each step age by the inverse of its variance to arrive at a weighted mean. The calculated mean more closely reflects, then, the more precisely determined step ages. Second, we have weighted each step by the proportion of the total gas (% ^{39}Ar) represented by that step, without allowing for differences in analytical errors. The second approach is more conservative in that the calculated standard deviations are larger than for the first approach; therefore, we will use the second set of plateau ages in subsequent discussion. However, there is no statistical difference (at the 1σ confidence level) between the two sets of plateau ages.

We used $^{36}\text{Ar}/^{40}\text{Ar}$ vs. $^{39}\text{Ar}/^{40}\text{Ar}$ correlation diagrams to determine isochron ages. Unlike the age spectrum plots that assume an initial $^{40}\text{Ar}/^{36}\text{Ar}$ composition equal to atmosphere, the correlation diagrams allow determination of the sample age and initial $^{40}\text{Ar}/^{36}\text{Ar}$ composition independently (see McDougall and Harrison, 1988, for a recent discussion). In such diagrams, only those steps that are collinear are used. For all samples, we found a $^{40}\text{Ar}/^{36}\text{Ar}$ intercept near the atmospheric composition (which is not surprising given that the rocks crystallized near or above sea level). The goodness-of-fit parameter SUMS (York, 1969) has a χ^2 distribution with (*N* - 2) degrees of freedom, *N* being the number of steps included. For reference, a value for SUMS/(*N* - 2) = 2.6 for a regression fit with five plateau steps would indicate that an isochron relationship for the step argon compo-

sitions could not be dismissed at the 95% confidence limit. Experiments that yield such an acceptable measure of the goodness of fit, near atmospheric $^{40}\text{Ar}/^{36}\text{Ar}$ intercept, and relatively concordant isochron and plateau ages are likely to have identified reliable crystallization ages (Lanphere and Dalrymple, 1978).

DISCUSSION OF AGE DETERMINATIONS

The $^{40}\text{Ar}/^{39}\text{Ar}$ incremental heating experiments have produced disturbed age spectra for samples from all sites but NB-1 (Figs. 2-7). Spurious step ages generally resulted from gas released at low temperatures, which we attribute to nonconcordant loss of radiogenic ^{40}Ar (during alteration) and ^{39}Ar (during neutron irradiation) from alteration minerals. A few samples (115-713A-15R-4, 43-47 cm, and 115-715A-29R-2, 32-35 cm) showed reactor-induced ^{39}Ar recoil effects (Turner and Cadoogan, 1974; Huneke and Smith, 1976), which produces erroneously young ages for (K-poor) high-temperature steps in fine-grained samples. The middle-to-high temperature portions of the gas released, however, generally displayed "acceptable" (albeit somewhat irregular) plateaus. Integrated ages, calculated by recombining the argon compositions of all steps (Table 1), are generally concordant with the plateau and isochron ages, indicating that ^{39}Ar has not been lost from the samples but has been redistributed within the mineral phases by irradiation recoil. Exceptions (115-707C-25R-1, 104-106 cm, and 115-707C-28R-4, 133-136 cm) are samples that have probably lost radiogenic ^{40}Ar and gained K during alteration of glassy groundmass to clays (Dalrymple and Clague, 1976; Seidemann, 1978). With the exception of the single sample from well NB-1, which yielded an unambiguous age spectrum, we have the results from several samples at each site to compare for consistency. Finally, very similar ages have been measured in two laboratories with different instruments and reactors, which reassures us that systematic experimental errors have been properly assessed.

Walker and McDougall (1982) have shown the utility in calculating Ca/K ratios from the $^{37}\text{Ar}/^{39}\text{Ar}$ compositions of individual gas increments to indicate the minerals responsible for the release of argon from the whole-rock samples within given temperature intervals. Mineralogic data from basaltic rocks from

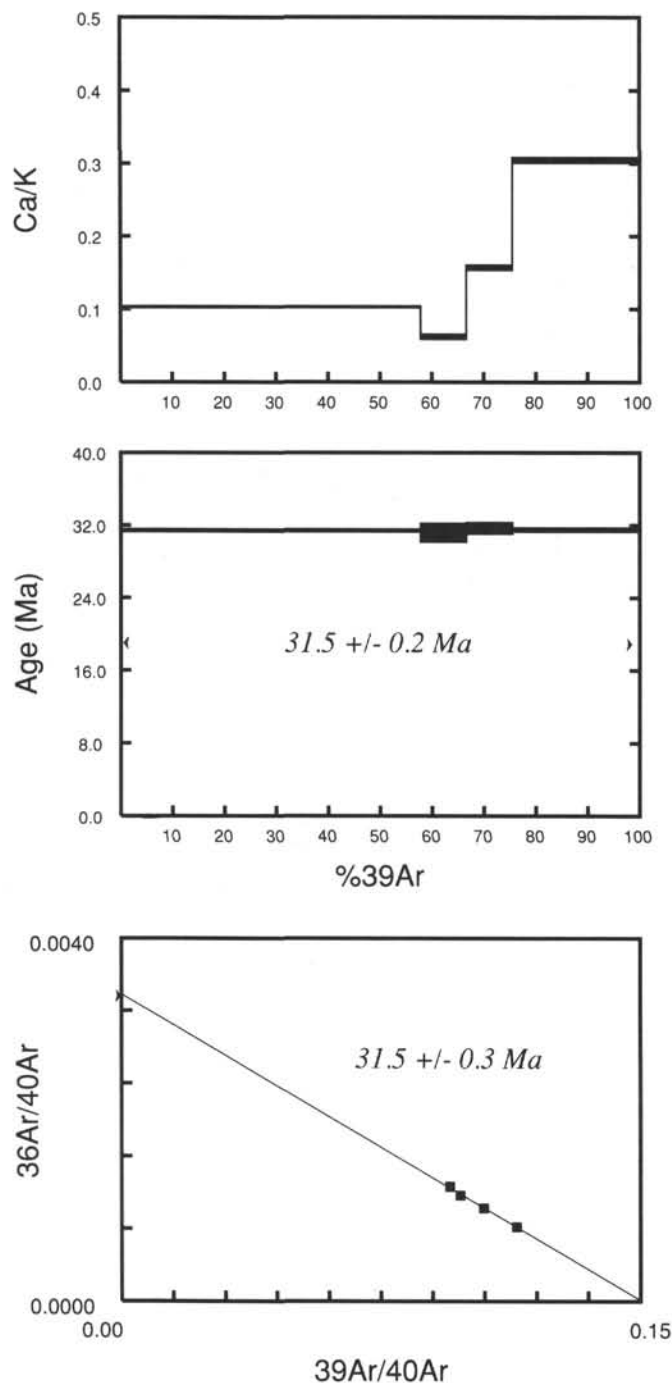


Figure 2. Apparent Ca/K and age release diagrams (above), and $^{36}\text{Ar}/^{40}\text{Ar}$ - $^{39}\text{Ar}/^{40}\text{Ar}$ isochron diagram (below) for trachyte Sample NB-1 from the Nazareth Bank. Horizontal boxes in the gas release plots indicate the estimated analytical error (± 1 SE) about each calculated Ca/K or step age. A plateau age (indicated) has been determined from the weighted mean of contiguous, concordant, gas increment ages. The isochron age has been determined from the best-fitting line to collinear gas-increment compositions (filled squares) after York (1969). Analytical uncertainties (± 1 SE) are shown; the atmospheric composition of argon is plotted on the ordinate.

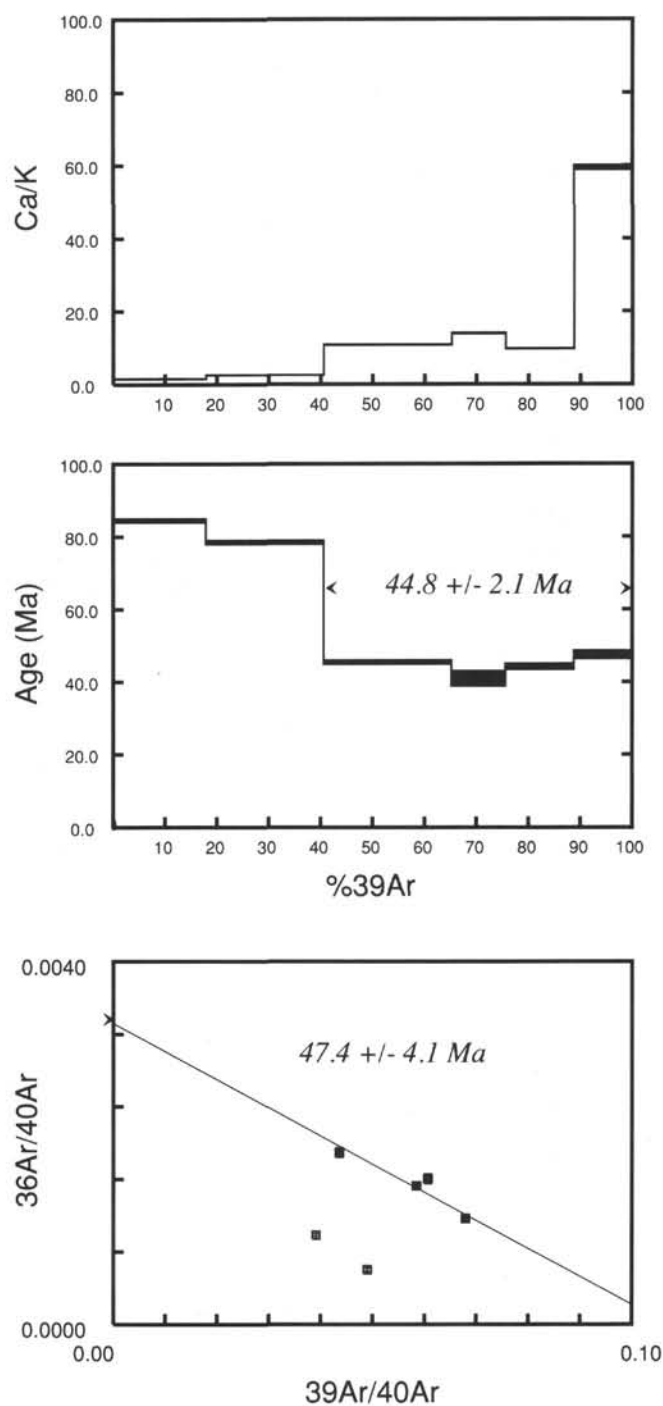


Figure 3. Apparent Ca/K and age release diagrams (above), and $^{36}\text{Ar}/^{40}\text{Ar}$ - $^{39}\text{Ar}/^{40}\text{Ar}$ isochron diagram (below) for basalt Sample SM-1-1 from the Saya de Malha Bank. Details as in Figure 2.

these sites (Fisk and Howard, this volume) show the range in Ca/K expected for the phases constituting these whole-rock samples: clinopyroxene (500–2000), plagioclase feldspar (20–500), glass (5–20), and clays (0.1–5). Plots of Ca/K vs. $\%^{39}\text{Ar}$ for our experiments (Figs. 2–7) show Ca/K increasing with temperature from values < 1 to > 300 . Basaltic samples (e.g., 115-706C-5R-1, 71–74 cm; Fig. 4) released argon from phases with Ca/K = 1–5 at low temperatures, indicative of clay alteration phases (smectite, celadonite). Middle temperature steps show Ca/K = 10–

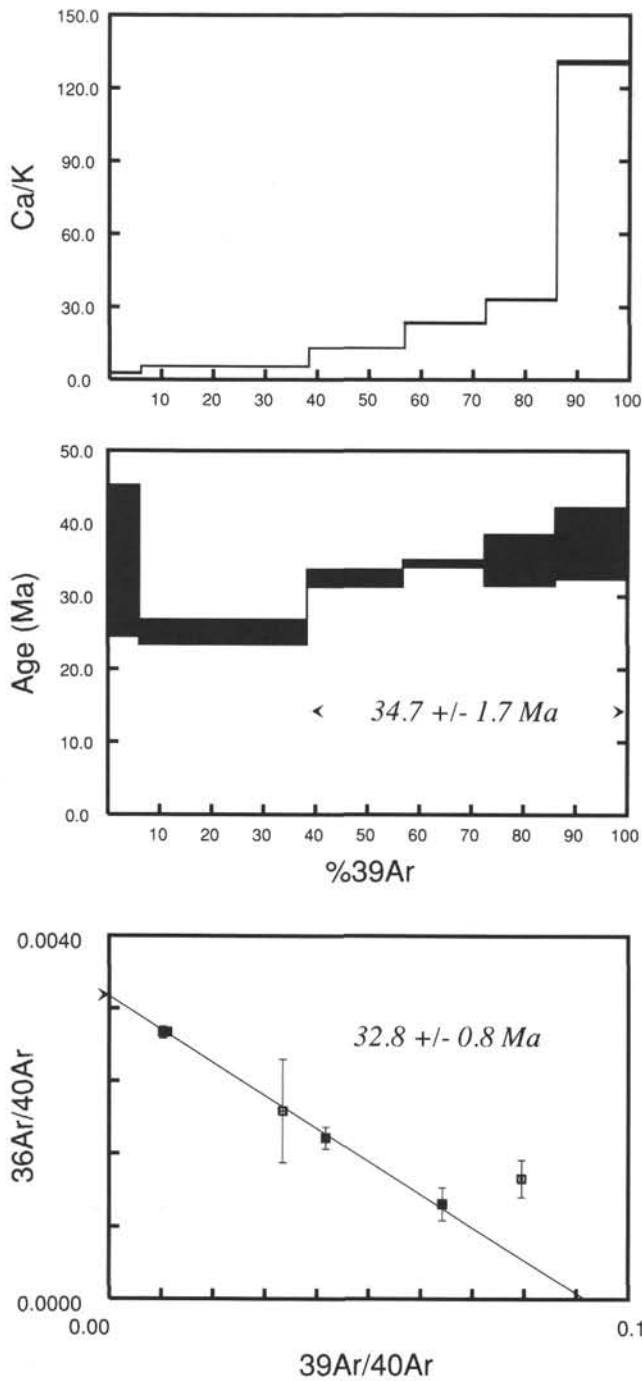


Figure 4. Apparent Ca/K and age release diagrams (above), and $^{36}\text{Ar}/^{40}\text{Ar}$ - $^{39}\text{Ar}/^{40}\text{Ar}$ isochron diagram (below) for basalt Sample 115-706C-5R-1, 71-74 cm, from the northeastern margin of the Mascarene Plateau. Details as in Figure 2.

60, from which we infer argon release from fresh glass and feldspar. At high temperatures ($\text{Ca}/\text{K} = 100\text{--}300$), gas was released primarily from feldspar. There appears to be very little ^{39}Ar contribution from pyroxenes, because of the low potassium content of that mineral. (Sample NB-1 is a trachyte composed predominantly of K-feldspar, which accounts for the narrow range in Ca/K in the release spectrum.) The gas increments that define the plateau ages, then, were released strictly from the igneous phases within the samples and so constitute crystallization ages.

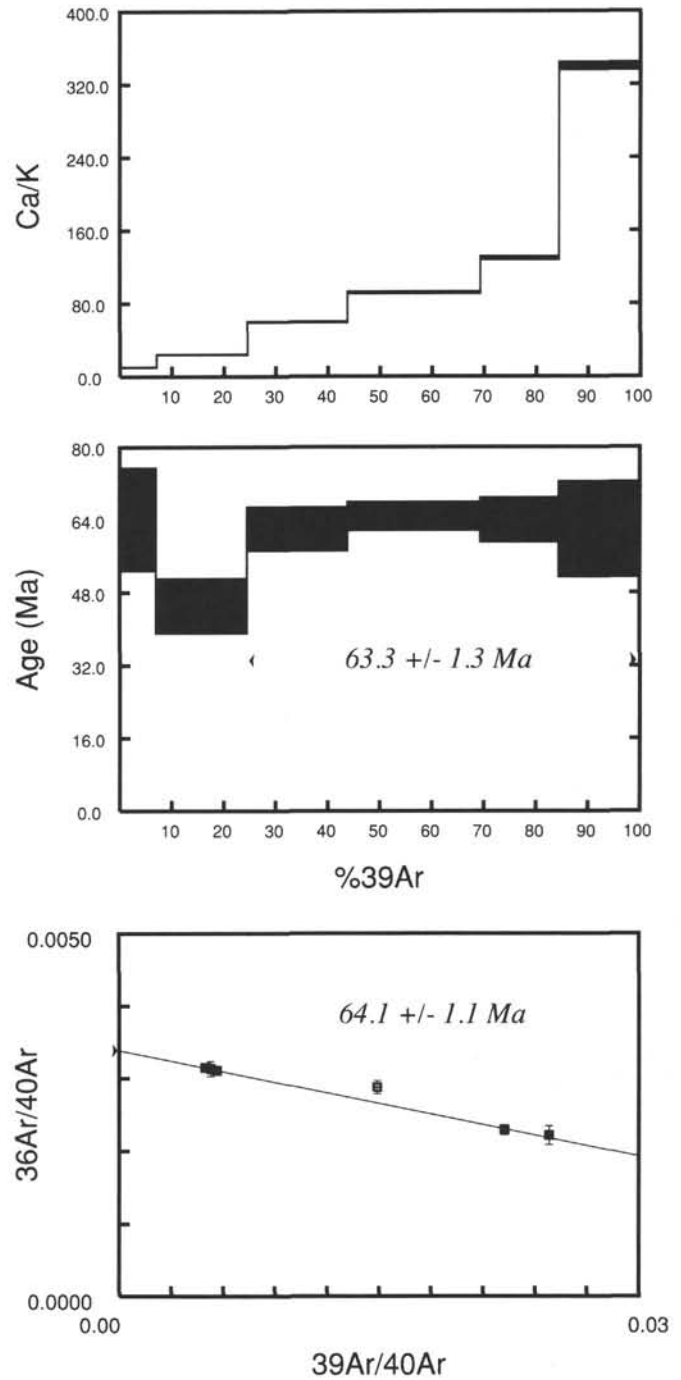


Figure 5. Apparent Ca/K and age release diagrams (above), and $^{36}\text{Ar}/^{40}\text{Ar}$ - $^{39}\text{Ar}/^{40}\text{Ar}$ isochron diagram (below) for basalt Sample 115-707C-26R-5, 110-113 cm, from the northern margin of the Mascarene Plateau. Details as in Figure 2.

Experiments on 18 samples from the six locations produced acceptable crystallization ages. In all cases, plateau ages (weighted by $\%^{39}\text{Ar}$) and isochron ages are concordant. We note that there are no significant differences (at the 1σ confidence limit) among the calculated sample ages at each site. Therefore, we may pool the individual sample ages to calculate a weighted-mean site age (weighted by the inverse variance of each sample age) from both plateau and isochron age estimates (Table 2). The site plateau ages, from south to north, are as follows: well

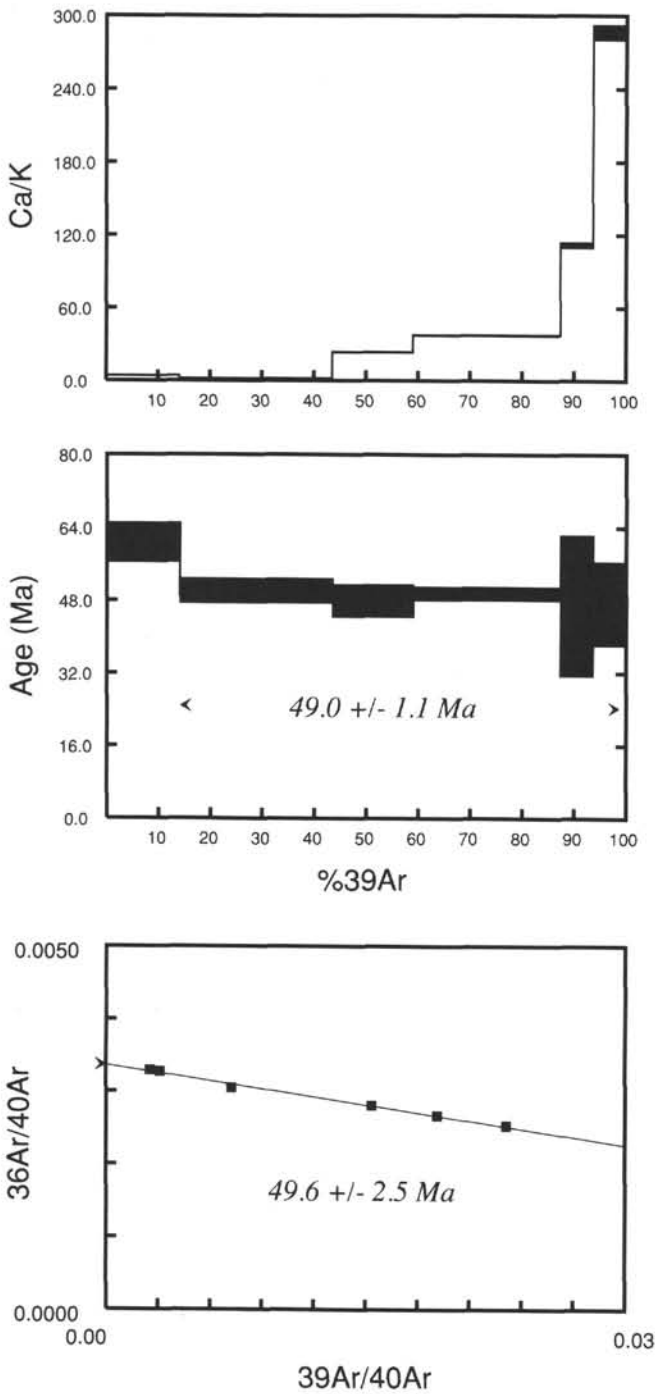


Figure 6. Apparent Ca/K and age release diagrams (above), and $^{36}\text{Ar}/^{40}\text{Ar}$ - $^{39}\text{Ar}/^{40}\text{Ar}$ isochron diagram (below) for basalt Sample 115-713A-15R-2, 62–65 cm, from the northern Chagos Bank. Details as in Figure 2.

site NB-1 (31.5 ± 0.2 Ma, $N = 1$); Site 706 (33.4 ± 0.5 Ma, $N = 4$); well site SM-1 (45.5 ± 1.9 Ma, $N = 2$); Site 707 (63.2 ± 1.3 Ma, $N = 3$); Site 713 (49.0 ± 1.0 , $N = 5$); and Site 715 (56.8 ± 1.8 Ma, $N = 3$). The site isochron ages are indistinguishable from these (Table 2), which reflects the atmospheric composition of the fitted $^{40}\text{Ar}/^{36}\text{Ar}$ intercepts (Table 1).

There is an unequivocal progression of increasing age of volcanic activity northward along the ridge system, connecting young oceanic-island volcanism at Réunion and Mauritius with flood basalt volcanism in India at Late Cretaceous/early Ter-

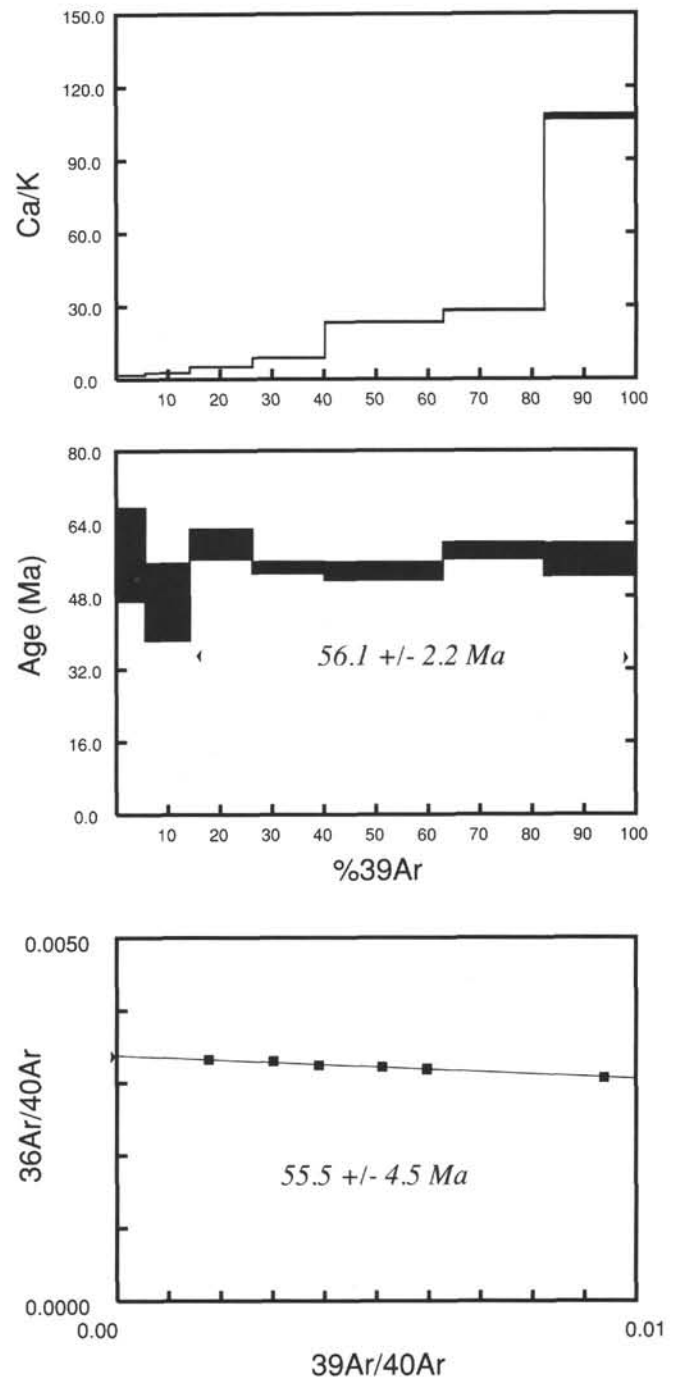


Figure 7. Apparent Ca/K and age release diagrams (above), and $^{36}\text{Ar}/^{40}\text{Ar}$ - $^{39}\text{Ar}/^{40}\text{Ar}$ isochron diagram (below) for basalt Sample 115-715A-30R-5, 132–135 cm, from the eastern margin of the Maldives Ridge. Details as in Figure 2.

tiary time (Fig. 8). This is strong confirmation of the hotspot model for the formation of this volcanic lineament. Indeed, the radiometric ages match closely with the age distribution of volcanism predicted from computer calculations of plate motions over an assumed stationary Réunion hotspot (Duncan, this volume).

Volcanism at Site 706 was contemporaneous with nascent seafloor spreading at the Central Indian Ridge, which began the present phase of northeast-southwest separation at Chron 13N time (35.3 – 35.9 Ma; Berggren et al., 1985b). Biostratigraphic

Table 2. Summary of weighted mean site ages, Réunion hotspot track.

Site	Samples (N)	Weighted mean of plateau ages	Weighted mean of isochron ages
706	4	33.4 ± 0.5	32.9 ± 0.7
707	3	63.2 ± 1.3	64.1 ± 1.1
713	5	49.0 ± 1.0	49.6 ± 0.6
715	3	56.8 ± 1.8	57.5 ± 2.5
NB-1	1	31.5 ± 0.2	31.5 ± 0.3
SM-1	2	45.5 ± 1.9	47.5 ± 3.6

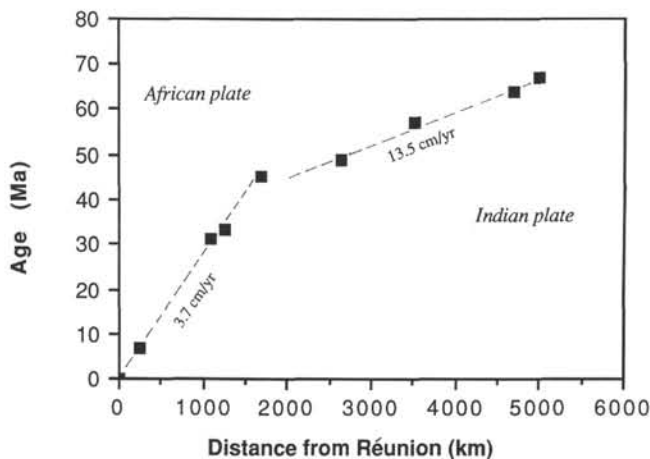


Figure 8. Age vs. distance for sites along the Réunion hotspot track from published data (McDougall, 1971; Duncan and Pyle, 1988) and new age determinations presented here (Table 2). Note the change in volcanic propagation rate when the Indian-African plate boundary (Central Indian Ridge) crossed over the hotspot. Before this event, the Indian Plate moved over the hotspot at about 13.5 cm/yr, whereas the African Plate has moved at about 3.7 cm/yr since.

data indicated an age for sediment interbedded with the basalt of lowermost Oligocene (Subzone CP16b or CP16c), or 33.8–35.9 Ma (Berggren et al., 1985b). Shipboard paleomagnetic measurements established that the basalts at Site 706 were uniformly normally magnetized whereas the overlying sediments were predominantly reversely magnetized, which would correspond to a Chron 12R–13N magnetostratigraphic assignment. Our best estimate for the basalt crystallization age (33.2 ± 0.5 Ma) is somewhat younger than the Berggren et al. (1985b) age range for Chron 13N, but it does corroborate the recently proposed adjustments of the Eocene/Oligocene boundary to 34.4 ± 0.6 Ma (Glass et al., 1986) and 33.7 ± 0.4 Ma (Montanari et al., 1988).

The tholeiitic basalts at Site 707, well to the west of the main hotspot track, were erupted at 63.7 ± 1.1 Ma. The biostratigraphic data at this site indicate that the oldest sediments are from the late part of the early Paleocene or the early part of the late Paleocene. The uniformly reversed polarity of the basalts could fit with Chrons 26R or 27R (60.8–63.0 or 63.5–64.3 Ma; Berggren et al., 1985a). Seafloor spreading between India and the Seychelles Bank began with a northward ridge jump at Chron 27N (63 Ma; Schlich, 1982) when Site 707 was adjacent to the western margin of India. The age of basalts at Site 707 overlaps with the younger $^{40}\text{Ar}/^{39}\text{Ar}$ incremental heating ages for Deccan basalts (Pande et al., 1988). Further geochemical work may allow correlation of Site 707 basalts with specific units within the

Deccan sequence. However, from its age and reconstructed position, we conclude that volcanism at Site 707 occurred somewhat after the main pulse of Deccan flood basalt activity, during early rifting of the Seychelles Bank from India at the nascent Carlsberg spreading ridge.

Volcanic activity at Site 713 built up a shallow submarine edifice at 49.3 ± 0.6 Ma. Baked sediments interbedded with these basalts are precisely assigned to Subzone CP13b, early-middle Eocene age. All basalt units were reversely magnetized, consistent with assignment to Chron 20R (Berggren et al., 1985a). Basalts at well site SM-1 are less precisely dated (44.8 ± 1.5 Ma), but they appear to be roughly contemporaneous with Site 713 basalts. When the Central Indian Ocean is reconstructed to middle Eocene time (McKenzie and Sclater, 1971), the Chagos and Saya de Malha banks are joined and could then be contemporaneous volcanic structures. This larger than usual accumulation of basalts may have formed when the hotspot lay beneath or close to a segment of the Paleogene Central Indian spreading ridge. Geochemical data are consistent with this interpretation (Baxter, this volume).

Site 715 basalts were erupted subaerially, at an oceanic island, at 57.2 ± 1.8 Ma. Biostratigraphic data indicated a late early Eocene age for the lowermost shallow-water carbonate sediments (Backman, Duncan, et al., 1988), which is several million years younger than the basalts. This difference may be explained by the time necessary for the island to subside below sea level. Indications from the geochemical data for Site 715 basalts (Baxter, this volume) are that this volcanism occurred well removed from a spreading ridge.

CONCLUSIONS

Concordant plateau and isochron ages have been established from the $^{40}\text{Ar}/^{39}\text{Ar}$ incremental heating experiments on volcanic rocks from six drilling sites along the Réunion hotspot track. This greatly expands the coverage of this volcanic lineament, previously sampled only at subaerial exposures.

The ages determined show a clear north-to-south progression that confirms the hotspot model for the volcanic origin of the collinear Mascarene Plateau, Chagos Bank, and Maldives-Laccadives ridges. Together with new ages from Leg 121 drilling on the parallel Ninetyeast Ridge, this temporal variation will be used to describe in detail the motion of plates bordering the Indian Ocean in the fixed hotspot reference frame.

Volcanic activity at Site 707, east of the Seychelles Bank, is associated with terminal eruptions of the Deccan basalts and early rifting of the Carlsberg spreading ridge. Precise biostratigraphic age assignments for sediments interbedded with dated basalts from Sites 706 and 713 will allow improvements in the magnetobiostratigraphic time scale.

ACKNOWLEDGMENTS

We thank Texaco, Inc., for providing volcanic material from Mascarene Plateau exploratory wells NB-1 and SM-1. K. Paulsen and L. Hogan assisted with $^{40}\text{Ar}/^{39}\text{Ar}$ analyses at Oregon State University. Neutron irradiation of samples at the OSU TRIGA reactor was helped by A. Johnson and T. Anderson. Analyses at Princeton were performed by R. Henne, and the data were massaged by T. C. Onstott and processed by D. L. Thompson. This research was supported by grants from JOI-USSAC.

REFERENCES

- Backman, J., Duncan, R. A., et al., 1988. *Proc. ODP. Init. Repts.*, 115: College Station, TX (Ocean Drilling Program).
- Baker, B. H., and Miller, J. A., 1963. Geology and geochronology of the Seychelles Islands and structures of the floor of the Arabian Sea. *Nature*, 199:346–348.

- Beane, J. E., Turner, C. A., Hooper, P. R., Subbarao, K. V., and Walsh, J. N., 1986. Stratigraphy, composition and form of the Deccan Basalts, Western Ghats, India. *Volcanology*, 48:1-33.
- Berggren, W. A., Kent, D. V., and Flynn, J. J., 1985a. Jurassic to Paleogene: Part 2. Paleogene geochronology and chronostratigraphy. In Snelling, N. J. (Ed.), *The Chronology of the Geological Record*. Geol. Soc. Mem. (London), 10:141-195.
- Berggren, W. A., Kent, D. V., and Van Couvering, J. A., 1985b. The Neogene: Part 2. Neogene geochronology and chronostratigraphy. In Snelling, N. J. (Ed.), *The Chronology of the Geological Record*. Geol. Soc. Mem. (London), 10:211-260.
- Courtillot, V., Besse, J., Vandamme, D., Montigny, R., Jaeger, J.-J., and Capetta, H., 1986. Deccan flood basalts at the Cretaceous/Tertiary boundary? *Earth Planet. Sci. Lett.*, 80:361-374.
- Courtillot, V., Féraud, G., Maluski, H., Vandamme, D., Moreau, M. G., and Besse, J., 1988. Deccan flood basalts and the Cretaceous/Tertiary boundary. *Nature*, 333:843-846.
- Cox, K. G., and Hawkesworth, C. J., 1985. Geochemical stratigraphy of the Deccan Traps at Mahabaleshwar, Western Ghats, India, with implications for open system magmatic processes. *J. Petrol.*, 26:355-377.
- Dalrymple, G. B., and Clague, D. A., 1976. Age of the Hawaiian-Emperor Bend. *Earth Planet. Sci. Lett.*, 31:317-321.
- Dalrymple, G. B., Clague, D. A., Vallier, T. L., and Menard, H. W., 1988. $^{40}\text{Ar}/^{39}\text{Ar}$ age, petrology, and tectonic significance of some seamounts in the Gulf of Alaska. In Keating, B. H., Fryer, P., Batiza, R., and Boehlert, G. W. (Eds.), *Seamounts, Islands and Atolls*. Am. Geophys. Union Monogr., 43:297-315.
- Dalrymple, G. B., and Lanphere, M. A., 1969. *Potassium-Argon Dating*: San Francisco (W. H. Freeman).
- Dalrymple, G. B., Lanphere, M. A., and Clague, D. A., 1981. Conventional and $^{40}\text{Ar}/^{39}\text{Ar}$ K-Ar ages of volcanic rocks from Ōjin (Site 430), Nintoku (Site 432), and Suiko (Site 433) seamounts and the chronology of volcanic propagation along the Hawaiian-Emperor Chain. In Jackson, E. D., Koizumi, I., et al., *Init. Repts. DSDP*, 55: Washington (U.S. Govt. Printing Office), 659-676.
- Duncan, R. A., 1981. Hotspots in the southern oceans—an absolute frame of reference for motion of the Gondwana continents. *Tectonophysics*, 74:29-42.
- Duncan, R. A., and Pyle, D. G., 1988. Rapid eruption of the Deccan flood basalts at the Cretaceous/Tertiary boundary. *Nature*, 333:841-843.
- Fisher, R. L., Johnson, G. L., and Heezen, B. C., 1967. Mascarene Plateau, western Indian Ocean. *Geol. Soc. Am. Bull.*, 78:1247-1266.
- Glass, B. P., Hall, C. M., and York, D., 1986. $^{40}\text{Ar}/^{39}\text{Ar}$ dating of North American tektite fragments from Barbados and the age of the Eocene/Oligocene boundary. *Chem. Geol.*, 59:181-186.
- Huneke, J. C., and Smith, S. P., 1976. The realities of recoil; ^{39}Ar recoil out of small grains and anomalous age patterns in $^{39}\text{Ar}/^{40}\text{Ar}$ dating. *Geochim. Cosmochim. Acta, Suppl.*, 7:1987-2008.
- Lanphere, M. A., and Dalrymple, G. B., 1978. The use of $^{40}\text{Ar}/^{39}\text{Ar}$ data in evaluation of disturbed K-Ar systems. In Zartman, R. E. (Ed.), *Short Papers of the Fourth International Conference, Geochronology, Isotope Geology*. U.S. Geol. Surv. Open-File Rep., 78-701, 241-243.
- McDougall, I., 1971. The geochronology and evolution of the young oceanic island of Réunion, Indian Ocean. *Geochim. Cosmochim. Acta*, 35:261-270.
- McDougall, I., and Harrison, T. M., 1988. *Geochronology and Thermochronology by the $^{40}\text{Ar}/^{39}\text{Ar}$ Method*: Oxford (Oxford Univ. Press).
- Macintyre, R. M., Dickin, A. P., Fallick, A. E., and Halliday, A. N., 1985. An isotopic and geochronological study of the younger igneous rocks of the Seychelles. *Eos*, 66:1137.
- McKenzie, D. P., and Sclater, J. G., 1971. The evolution of the Indian Ocean since the Late Cretaceous. *Geophys. J. R. Astron. Soc.*, 25: 437-528.
- Mahoney, J. J., 1988. Deccan Traps. In Macdougall, J. D. (Ed.), *Continental Flood Basalts*: Dordrecht, The Netherlands (Kluwer Academic Publishers), 151-194.
- Masliwec, A., 1981. The direct dating of ore minerals [M.S. thesis]. Univ. Toronto, Toronto, Canada.
- Meyerhoff, A. A., and Kamen-Kaye, M., 1981. Petroleum prospects of the Saya de Malha and Nazareth banks, Indian Ocean. *AAPG Bull.*, 65:1344-1347.
- Montanari, A., DePaolo, D. J., Drake, R., Alvarez, W., Deino, A., Curtis, G. H., Odin, G. S., Turrin, B. D., and Bice, D. M., 1988. Radio-isotopic calibration of the upper Eocene and Oligocene magnetic polarity and foraminiferal time scales in the northern Apennines of Italy. *Geol. Soc. Am., Abstr. Programs*, 20:a178.
- Morgan, W. J., 1972. Plate motions and deep mantle convection. *Mem. Geol. Soc. Am.*, 132:7-22.
- , 1978. Rodrigues, Darwin, Amsterdam—a second type of hotspot island. *J. Geophys. Res.*, 83:5355-5360.
- , 1981. Hotspot tracks and the opening of the Atlantic and Indian Oceans. In Emiliani, C. (Ed.), *The Sea* (Vol. 7): *The Oceanic Lithosphere*: New York (Wiley-Interscience), 443-487.
- Pande, K., Verikatesan, T. R., Gopalan, K., Krishnamurthy, P., and Macdougall, J. D., 1988. $^{40}\text{Ar}/^{39}\text{Ar}$ ages of alkali basalts from Kutch, Deccan Volcanic Province, India. In Subbarao, K. V. (Ed.), *Workshop on Deccan Flood Basalts*. Geol. Soc. India, 9:145-150.
- Richards, M. A., Duncan, R. A., and Courtillot, V., in press. Flood basalts and hotspot tracks: plume heads and tails.
- Samson, S. D., and Alexander, E. C., Jr., 1987. Calibration of the inter-laboratory $^{40}\text{Ar}/^{39}\text{Ar}$ dating standard, MMhb-1. *Chem. Geol.*, 66: 27-34.
- Schlich, R., 1982. The Indian Ocean: aseismic ridges, spreading centers and oceanic basins. In Nairn, A.E.M., and Stehli, F. G. (Eds.), *The Sea* (Vol. 6): *The Ocean Basins and Margins*: New York (Plenum Press), 51-147.
- Seidemann, D. E., 1978. $^{40}\text{Ar}/^{39}\text{Ar}$ studies of deep sea igneous rocks. *Geochim. Cosmochim. Acta*, 42:1721-1734.
- Turner, G., and Cadogan, P. H., 1974. Possible effects of ^{39}Ar recoil in $^{40}\text{Ar}/^{39}\text{Ar}$ dating of lunar samples. *Geochim. Cosmochim. Acta, Suppl.*, 5:1601-1615.
- Walker, D. A., and McDougall, I., 1982. $^{40}\text{Ar}/^{39}\text{Ar}$ and K-Ar dating of altered glassy volcanic rocks: the Dabi Volcanics, P.N.G. *Geochim. Cosmochim. Acta*, 46:2181-2190.
- York, D., 1969. Least-squares fitting of a straight line with correlated errors. *Earth Planet. Sci. Lett.*, 5:320-324.

Date of initial receipt: 31 March 1989

Date of acceptance: 28 November 1989

Ms 115B-141